*Cone Penetration Testing 2022 – Gottardi & Tonni (eds)*


# Undrained strength from CPTu in brittle soils: A numerical perspective

L. Monforte, M. Arroyo & A. Gens
*CIMNE-UPC, Barcelona, Spain*

ABSTRACT: Static liquefaction of soils that have a brittle undrained response (hydraulic fills, mine tailings or sensitive clays) may lead to sudden failures of large consequence. Given the importance of undrained failure, obtaining precise estimates of peak and residual yield strength is important. The CPTu plays a major role in the geotechnical characterization of these geomaterials and so do CPTu-based estimates of undrained strength. Most of the methods available for CPTu-based estimation of undrained strength are empirical, based on correlation with other laboratory or field tests. When such correlations are established difficulties appear due to variable disturbance affecting the reference laboratory samples and parasitic effects, such as unaccounted for partial drainage during penetration or unknown side friction, affecting the cone results. Such difficulties are not present when using numerical simulation. The paper builds upon a series of CPTu simulations using a model able to represent brittle undrained failure. Confounding factors such as partial drainage and cone side friction are systematically varied to examine their effect on the results. The results are then employed to examine the performance of several empirical methods frequently employed to obtain peak and residual strength from CPTu.

## 1 INTRODUCTION

Some geomaterials (hydraulic fills, mine tailings or sensitive clays) may exhibit undrained softening upon shearing (static liquefaction): a drastic decrease of the effective mean stress and mobilized undrained shear strength. Static liquefaction is a brittle response that may lead to catastrophic sudden failures, often associated with loss of life and major environmental impact (Gens, 2019). The identification and characterization of these materials is therefore of paramount importance.

The extraction of good-quality samples of these loose/soft soils is challenging and in situ tests are essential for their characterization (Been, 2016; Gens 2019). The interpretation of CPTu soundings in these brittle materials is not always straightforward, particularly as their permeability does frequently result in partly drained conditions (Schnaid, 2021). Nevertheless, several correlations are in use to relate cone metrics and peak and residual undrained shear strength in brittle soils.

Numerical simulation of CPT may offer new insights of the mechanisms during insertion, leading to more reliable interpretation techniques. To this end, Monforte et al (2021) reported a parametric analysis employing the Particle Finite Element method (PFEM) in which several materials with different idealized materials of variable undrained brittleness were considered in the simulation of CPTu. The analysis also assessed the effect of drainage conditions and interface friction angle on cone metrics. In this work we exploit the simulation database of Monforte et al (2021) to assess several cone interpretation techniques frequently employed in current practice to infer undrained strength.

## 2 NUMERICAL DATABASE

### 2.1 *Simulation method*

Numerical simulations (Monforte et al, 2021) have been carried out by means of G-PFEM (Geotechnical Particle Finite Element Method), specially designed for the analysis of problems involving the penetration of rigid structures into fluid-saturated soil masses (Monforte et al, 2017, 2018).

The cone has standard dimensions and is assumed rigid. CPT symmetry allows for an axisymmetric model. The stress state is set up by prescribing a vertical stress of 96 kPa at the top boundary and of 56 kPa at the radial boundary, i.e. a $K_0$ value of 0.58. The CPT is advanced by 30 diameters into the soil attaining a steady state in all the simulated records.

### 2.2 *Materials simulated*

The soil is described by a version of the Clay and Sand Model (CASM) (Yu, 1998; Manica et al. 2021; Arroyo & Gens, 2021). Common constitutive parameters for all cases examined are reported in Table 1. Materials with different brittleness index are obtained by modifying the geometry of the yield surface (shape

DOI: 10.1201/9781003308829-85

parameter, $n$, and spacing ratio, $r$), see Table 2. Because of these choices all the simulated materials share the same normal compression line, but their critical state line has different positions on the compression plane. In undrained conditions, all materials share the same peak undrained shear strength, whereas the residual undrained shear strength varies (Table 2).

Example triaxial responses after anisotropic ($K_0$) consolidation are reported in Figure 1. In undrained conditions, after reaching the peak, deviatoric stresses reduce due to strain softening; material A is the most brittle whereas material H is almost insensitive.

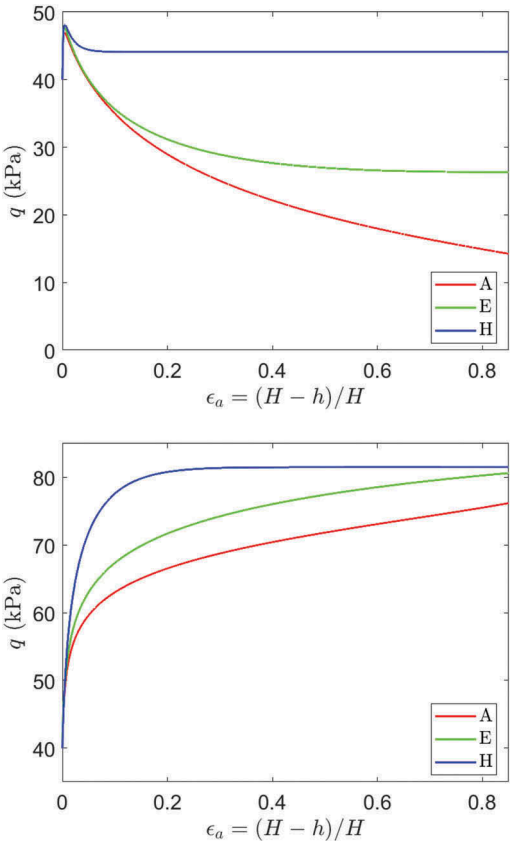


Figure 1. K0 triaxial compression behavior of materials A, E and H: undrained loading, top, and drained loading, bottom.

### 2.3 *Parametric study*

For every CASM material, the parametric analysis presented below examines the effect of drainage conditions and soil-cone interface friction angle. Drainage conditions are controlled through permeability values, which have been varied between $10^{-9}$ m/s and $10^{-3}$ m/s. To avoid clutter most results below are only presented for three values: $10^{-8}$ m/s (fully undrained), $10^{-6}$ m/s (partly drained) and $10^{-3}$ m/s (fully drained).

The interface friction angles employed ($\delta = 0, 7°, 12°$ and $19°$) correspond to interface efficiencies, tan ($\delta$)/tan ($\phi$), between 0 and 0.74, since the soil friction angle is 24º.

Currently, manufactured average roughness, $R_a$, for CPTu friction sleeves may lie between 0.65µm and 0.15µm (EN ISO 22476-1), in a range that aims to approach the roughness that may be later acquired upon use. For fine grained soils the resulting normalized roughness ($R_a/D_{50}$) will typically vary in the range ($10^{-3}$ to $10^{-1}$) that has been experimentally shown (Subba Rao et al. 2000; Eid et al. 2014) to result on interface efficiency between 0.3 and 0.9. On this basis the higher values of interface friction in the parametric study would be representative of testing on clays and fine silts, whereas the lower values would be more representative for testing on coarser silts and sands.

Table 1. Constitutive parameters common for all materials.

| $\kappa$ | $\lambda$ | $M$ | $G$ (kPa) | $K_0$ | $e_0$ | OCR |
|---|---|---|---|---|---|---|
| 0.016 | 0.053 | 0.98 | 3000 | 0.58 | 1 | 1 |

Table 2. Constitutive parameters varied.

| Material | $n$ | $r$ | $S_u^{peak}$ (kPa) | $S_u^{res}$ (kPa) | Ψ |
|---|---|---|---|---|---|
| A | 10 | 12 | 23.5 | 6.9 | 0.093 |
| E | 8 | 4 | 23.8 | 13.2 | 0.052 |
| H | 4 | 2 | 24 | 22.1 | 0.026 |

## 3 SIMULATION RESULTS AND CLASSIFICATION CHARTS

Figure 2 reports the results in two classification charts proposed by Robertson (1991; 2016). The 1991 chart is expressed using the following normalized parameters

$$Q_1 = \frac{q_t - \sigma_v}{\sigma'_{v0}} \quad B_q = \frac{u_2 - u_0}{q_t - \sigma_{v0}} \tag{1}$$

whereas the 2016 chart is expressed using the following normalized parameters

$$Q_{tn} = \left(\frac{q_t - \sigma_{v0}}{p_a}\right)\left(\frac{p_a}{\sigma'_{v0}}\right)^n \quad F_r = \frac{f_s}{q_t - \sigma_v} \tag{2}$$

where $n$ is an index, which is ultimately dependent on $Q_{tn}$ and $F_r$, and is established by iteration.

In the $B_q$ vs $Q_1$ classification graph the dominant effect is that of permeability. The undrained simulations have always $B_q > 0.5$, those drained have $B_q = 0$ and the partly drained ones lie in between. For impermeable materials brittleness plays also a significant

role, with material A (most brittle) generating the larger pore pressures. Interface friction has no systematic effect. According to this chart Material A will classify as sensitive, fine grained, if impermeable, as clay to silty clay if partly drained and as a silt mixture if fully drained.

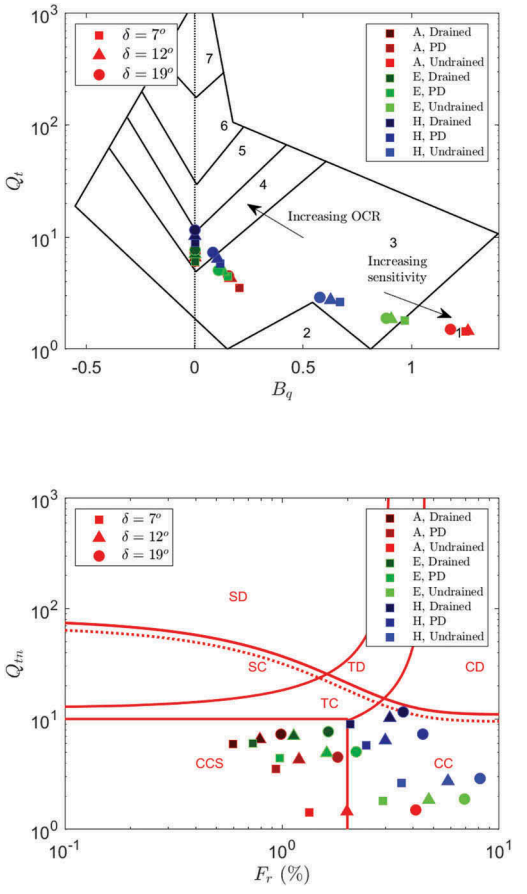


Figure 2. Results of the analyses of CPTu test with different permeabilities and interface friction angles plotted on classification charts. Above: Robertson 1991. Below: Robertson 2016. The marker color indicates undrained brittleness; marker shape indicates side friction values; marker hue indicates pemeability. PD = Partly drained.

In the $F_r$ vs $Q_{tn}$ classification graph all numerical results plot in the "contractive" zone, which is correct as none of the CASM materials were dilatant in shear. For material A most simulated results fall into the "sensitive" zone (CCS), which seems correct. However, this is also the case for material E if partly or fully drained, which seems excessive. There is also some disagreement with the graph when the effect of permeability is considered. Results for all materials and interface frictions shift upwards as permeability is increased. Although this is in line with the trend in the graph, even the fully drained material would classify as "clay-like" and be expected to behave in an undrained manner under CPTu. Finally, it is noticeable how changes on interface friction result in significant shifts along the $F_r$ axis for the same brittleness and permeability.

## 4 PEAK UNDRAINED SHEAR STRENGTH

### 4.1 *Cone factors*

One of the most frequent and important applications of the CPTu is to obtain estimates of peak undrained strength. The dominant approach uses empirically determined cone factors, that relate cone measurements and undrained strengths. Cone factors based on tip resistance and excess pore pressure are defined as

$$N_{kt} = \frac{q_t - \sigma_v}{s_u} \quad N_{\Delta u} = \frac{u_2 - u_0}{s_u} \tag{3}$$

It has been stressed many times (e.g. Mayne & Peuchen, 2018) that for this approach to make sense the target undrained strength of the correlation should be clearly specified. Peak undrained strengths measured on triaxial compression after anisotropic ($K_0$) consolidation are adopted here as a target, in line with previous work (e.g. Karlsrud et al. 2005). Another important factor (Lunne et al. 1997) is sample disturbance, as it will affect the laboratory values employed in correlations. Poor sample quality will typically decrease the undrained peak strength measured on the laboratory and thus increase empirically determined cone factors.

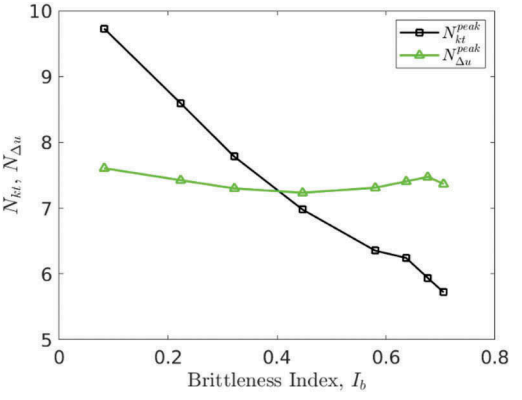


Figure 3. Cone factors for peak undrained strength in terms of the brittleness for smooth, undrained simulations.

Figure 3 reports the cone factors in terms of the brittleness index for smooth, undrained simulations. The tip resistance cone factor $N_{kt}$ is far more variable than the pore pressure cone factor $N_{\Delta u}$, something well in line with empirical observations (Lunne et al. 1997). Furthermore, the values of $N_{\Delta u}$ obtained from

these undrained smooth simulations cluster around the value 7.5, well supported by experimental work on Norwegian clays (Paniagua et al. 2019).

The advantage of $N_{\Delta u}$ as a more stable factor disappears when partial drainage is introduced in the picture (Figure 4). Excess pore pressure reduces and the cone factor required to recover peak undrained strength reduces accordingly. The effect of interface friction on this trend appears to be relatively small. The more realistic frictional simulations result on slightly smaller $N_{\Delta u}$ than the empirical average, something that may be explained by a small amount of sampling disturbance.

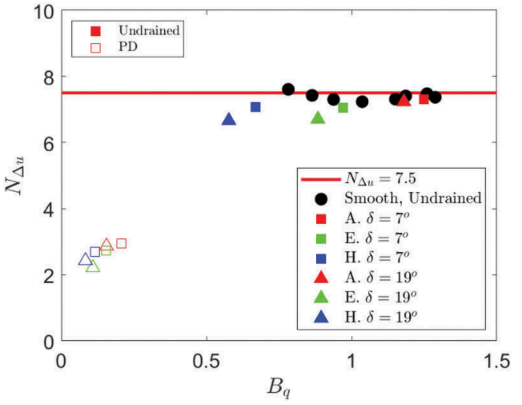


Figure 4. Simulation results and relations from literature between cone factor $N_{\Delta u}$ and pore pressure parameter $B_q$.

The variability of $N_{kt}$ is sometimes accounted for using $B_q$ as an auxiliary variable (Lunne et al. 1997; Mayne & Peuchen, 2018). Figure 5 presents the results for frictional undrained and partly drained simulations in that format. The results suggest that the higher cone factors that are sometimes obtained at low $B_q$ may be related to partial drainage. For fully undrained cases, it is also noteworthy that the cone factors for the less brittle material H are only slightly below the value ($N_{kt}$ = 12) that empirical studies assign to clays of moderate to low sensitivity (Low et al. 2010). As material brittleness is increased the simulated $N_{kt}$ cone factors reduce. The reduction observed is steeper than what data from general databases, such as that of Mayne & Peuchen (2018) would suggest. This difference is likely to be the result of increased sampling damage for the more brittle soils, something also borne out by the steeper decrease that was observed by Lunne et al (1997), using a more restricted dataset of higher sampling quality.

As noted by Karlsrud et al (2005) a relation between $N_{kt}$ and $B_q$ mediated by $N_{\Delta u}$ is just implied by their definition. According to the results just presented the undrained CASM simulations should then be fitted by

$$N_{kt} = \frac{N_{\Delta u}}{B_q} = \frac{7.5}{B_q} \tag{4}$$

Which is closely correct for the undrained results and far off the mark for partially drained cases (Figure 6).

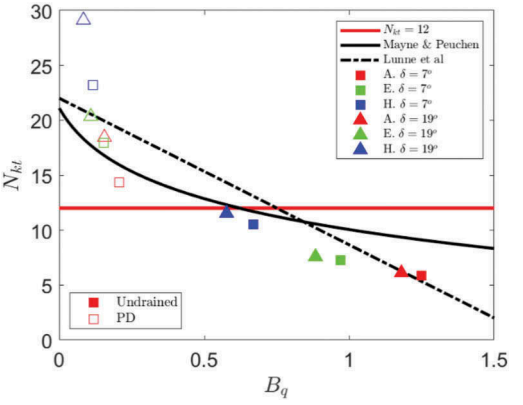


Figure 5. Simulation results and relations from literature between cone factor $N_{kt}$ and pore pressure parameter $B_q$.

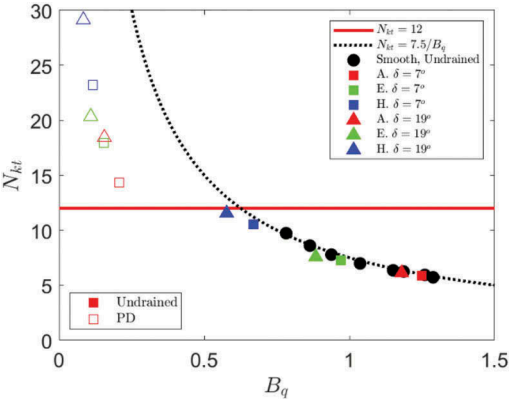


Figure 6. Simulation results and relations from literature between cone factor $N_{kt}$ and pore pressure parameter $B_q$.

### 4.2 *Case-history based correlations*

Olson & Stark (2003) back-analyzed case history data of flow liquefaction failures to obtain estimates of stress normalized undrained peak (yield) strength which were then correlated with the results of CPT. This correlation reads

$$\frac{S_u^{pk}}{\sigma'_{v0}} = 0.205 + 0.0143\ q_{c1} \pm 0.04 \tag{5}$$

$$q_{c1} = q_c \frac{1.8}{0.8 + \left(\frac{\sigma'_v}{p_a}\right)} \quad (6)$$

where the tip and corrected tip resistance $q_{c1}$ are expressed in MPa. The simulated CPT results lie in the range 0.14 to 1.14 $q_{c1}$ for which the correlation predicted upper bound of normalized peak strength is 0.21, only slightly below the input value.

## 5 RESIDUAL UNDRAINED SHEAR STRENGTH

### 5.1 *Sleeve friction*

Empirical observations of the close similitude of sleeve friction to residual undrained strength in clay as measured by vane tests or laboratory test on remolded soil are frequent (Lunne et al. 1997; Robertson, 2010). This can be simply expressed as

$$\frac{S_u^{res}}{\sigma'_{v0}} \approx \frac{f_s}{\sigma'_{v0}} \quad (7)$$

Figure 7 reports the normalized friction sleeve resistance of PFEM simulations in terms of the normalized residual undrained shear strength predicted by CASM; results are plotted for undrained and partly drained conditions. For high interface friction angles and undrained conditions, Equation (7) holds, and the friction sleeve is approximately equal to the residual undrained shear strength. For lower interface friction angles the tangential stress acting on the friction sleeve is lower than the residual undrained shear strength and Equation (7) becomes highly conservative. The importance of sleeve roughness for this correlation is thus clearly demonstrated. Interestingly, the effect of partial drainage is small for the more brittle material A, but large for the less brittle H.

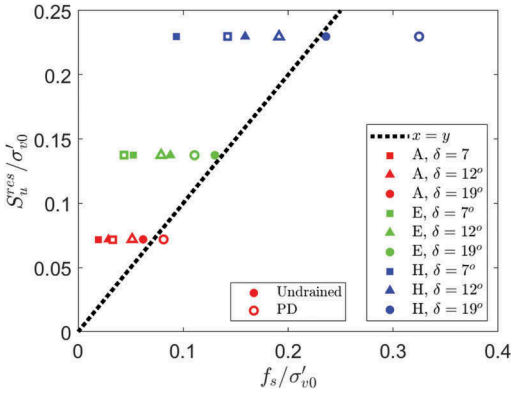


Figure 7. Residual undrained strength and side friction. All results correspond to practically undrained tests.

### 5.2 *Case-history based correlations*

Case-history back-analysis by Olson & Stark (2002) in which post-liquefaction geometry was considered led to another correlation of residual undrained strength with corrected tip resistance $q_{c1}$. Again, the correlation obtained has very little sensitivity to $q_{c1}$ in the range covered by our simulations and the predicted stress normalized residual (liquefied) undrained strength is practically constant. This is interesting, as the stress normalized residual strength is controlled by CASM material parameters and also constant for a given material type. The simulation results are above the recommended limits, but, for the most brittle material A, well within the values supporting the correlation (Figure 8). This comparison is unaffected by partial drainage or sleeve friction values. It is also worth mentioning that although material A is brittle, CASM has been fitted to represent even more brittleness when back-analyzing liquefaction failures (Arroyo & Gens, 2021; Mánica et al. 2021). Despite that Olson & Stark (2002) upper bound might still be somewhat conservative.

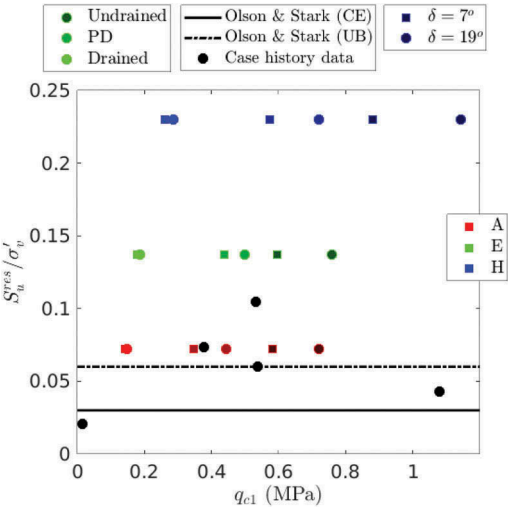


Figure 8. Comparison of the numerical results with case-history based correlation of Olson & Stark (2002).

Robertson (2010, 2021) also proposed correlations between residual undrained shear strength and cone metrics based on case history data. For materials with soil behavior type (SBT) index, $I_c > 3$ it is recommended to use the relation -discussed abovewith sleeve friction. For materials with SBT $I_c < 3$ a different relation was proposed. The soil behavior type index, $I_c$ is defined as

$$I_c = \left( (3.43 - \log Q_{tn})^2 + (\log F_r + 1.22)^2 \right)^{0.5} \quad (8)$$

The relation with undrained strength is based on $Q_{tn,cs}$ a corrected, "clean sand equivalent", value of normalized cone resistance $Q_{tn}$. This correction is given by:

$$Q_{tn,cs} = K_c \, Q_{tn} \tag{9}$$

The correction factor $K_c$ is itself also dependent (trough fifth-order polynomials) on $I_c$ .

Robertson relations (2010, 2021) are plotted in Figure 9 alongside the results for the fully drained simulations, which were the only ones resulting on $I_c$ < 3. The relations are postulated as lower bounds and the simulation results plot above them, except for a datapoint that represents high mobilized interface friction for soil H, which is almost non-brittle. For the higher brittleness case A, which is likely more similar to the soils in the database, the degree of conservatism implied by the relation does not appear excessive.

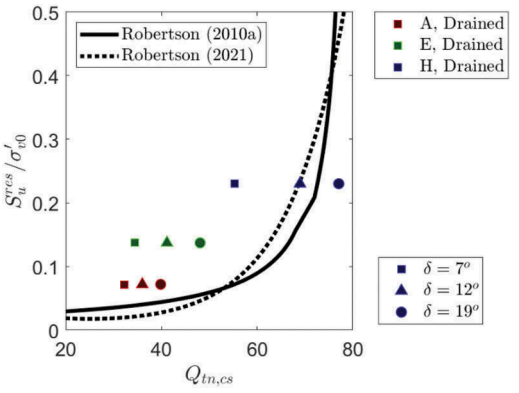


Figure 9. Comparison of numerical results with Roberston (2010, 2021) correlations for normalized residual undrained strength. The marker color indicates undrained brittleness; marker shape indicates side friction values; marker hue indicates permeability.

## 6 CONCLUSIONS

The ability to simulate CPTu response using realistic geometry and constitutive models is still relatively recent. If exploited systematically it will open a way to reduce the relatively large uncertainty that hinders empirically based correlations, by identifying which parasitic factors may be playing a role in some datasets and/or suggesting ways to adapt general correlations to the local soil characteristics.

This has been illustrated here for the case of soils with a brittle undrained response. The results indicate that partial drainage is a major factor when selecting cone factors for $s_{u\_pk}$. They also suggest that, when aiming for undrained residual strength, Olson & Stark (2002) proposals are more robust than Robertson (2010, 2021), as these are more sensitive to the possibility of partial drainage and -for fine grained soilsto the state of the cone-soil interface. Still, these results are based on a limited set of simulations and would require confirmation from more systematic parametric analyses.

## ACKNOWLEDGMENTS

The authors acknowledge financial support from the Spanish Ministry of Economy and Competitiveness, through the "Severo Ochoa Programme for Centres of Excellence in R&D" (CEX2018-000797-S).

## REFERENCES

Arroyo, M. & Gens, A. 2021. Computational analyses of Dam I failure at the Corrego de Feijao mine in Brumadinho, Final Report; available at http://www.mpf.mp.br/mg/sala-de-imprensa/docs/2021/relatorio-final-cinme-upc-1

Been, K. 2016. Characterizing mine tailings for geotechnical design. Australian Geomechanics, 51(4), 59–78.

Gens, A. 2019. Hydraulic fills with special focus on liquefaction. *Proceedings of the XVIII European Conference on Soil Mechanics and Geotechnical Engineering*.

Eid, H. T., Amarasinghe, R. S., Rabie, K. H. & Wijewickreme, D. 2014. Residual shear strength of fine-grained soils and soil–solid interfaces at low effective normal stresses. Canadian Geotechnical Journal, 52 (2),198 –210.

EN ISO 22476-1. 2012. Geotechnical investigation and testing. Field testing. Electrical cone and piezocone penetration test

Karlsrud, K., Lunne, T., Kort, D. A. & Strandvik, S. 2005. CPTU correlations for clays. In Proceedings of the 16th international conference on soil mechanics and geotechnical engineering (pp. 693–702). IOS Press.

Lunne, T., Robertson, P. K. & Powell, J. J. 1997. Cone penetration testing in geotechnical practice. CRC Press.

Low, H. E., Lunne, T., Andersen, K. H., Sjursen, M. A., Li, X., & Randolph, M. F. 2010. Estimation of intact and remoulded undrained shear strengths from penetration tests in soft clays. Géotechnique, 60(11), 843–859.

Mánica, M. A., Arroyo, M., Gens, A. & Monforte, L. 2021. Application of a critical state model to the Merriespruit tailings dam failure. Proceedings of the Institution of Civil Engineers - Geotechnical Engineering, 1–15.

Mayne, P. W. & Peuchen, J. 2018. Evaluation of CPTU Nkt cone factor for undrained strength of clays. In Cone Penetration Testing 2018 (pp. 423–429). CRC Press.

Monforte, L., Arroyo, M., Carbonell, J.M. & Gens, A. 2017. Numerical simulation of undrained insertion problems in geotechnical engineering with the particle finite element method (PFEM). *Computers and Geotechnics*. 82:144–156.

Monforte, L., Arroyo, M., Carbonell, J.M. & Gens, A. 2018. Coupled effective stress analysis of insertion problems in geotechnics with the particle finite element method. *Computers and Geotechnics*. 101:114–129.

Monforte, L., Gens, A., Arroyo, M., Mánica, M. & Carbonell, J.M. 2021. Analysis of cone penetration in brittle liquefiable soils. *Computers and Geotechnics*. 134:104123.

Olson, S. M. & Stark, T. D. 2002. Liquefied strength ratio from liquefaction flow failure case histories. Canadian Geotechnical Journal, 39(3), 629–647.

Olson, S. M. & Stark, T. D. 2003. Yield strength ratio and liquefaction analysis of slopes and embankments. Journal of Geotechnical and Geoenvironmental Engineering, 129(8), 727–737.

Paniagua, P., D'Ignazio, M., L'Heureux, J.-S., Lunne, T., Karlsrud, K. 2019. CPTU correlations for Norwegian clays: an update. AIMS Geosciences 2019, 5(2): 82–103

Robertson, P. K. 1991. Soil classification using the cone penetration test: Reply. Canadian geotechnical journal, 28(1), 176–178.

Robertson, P.K. 2010. Evaluation of flow liquefaction and liquefied strength using cone penetration test. *Journal of Geotechnical and Geoenvironmental Engineering*.136 (6): 842–853.

Robertson, P. K. 2016. Cone penetration test (CPT)-based soil behaviour type (SBT) classification system—an update. *Canadian Geotechnical Journal*, *53*(12), 1910–1927.

Robertson, P.K. 2021. Evaluation of flow liquefaction and liquefied strength using cone penetration test: an update. *Canadian Geotechnical Journal*. In press.

Schnaid, F. 2021. The Ninth James K. Mitchell Lecture: On the Geomechanics and Geocharacterization of Tailings. Int. Conf. On Site Charact., Budapest.

Subba Rao, K. S., Allam, M. M., & Robinson, R. G. 2000. Drained shear strength of fine-grained soil–solid surface interfaces. Proceedings of the Institution of Civil Engineers-Geotechnical Engineering, 143(2), 75–81.

Yu, H.S. 1998. CASM: a unified state parameter model for clay and sand. *International Journal for Numerical and Analytical methods in Geomechanics*. 22: 621–653.